2015

Nondestructive characterization of pipeline materials

Brady J. Engle
Iowa State University

Lucinda J. Smart
Iowa State University

Leonard J. Bond
Iowa State University, bondlj@iastate.edu

Nondestructive characterization of pipeline materials

Abstract

There is a growing need to quantitatively and nondestructively evaluate the strength and toughness properties of pipeline steels, particularly in aging pipeline infrastructure. These strength and toughness properties, namely yield strength, tensile strength, transition temperature, and toughness, are essential for determining the safe operating pressure of the pipelines. For some older pipelines crucial information can be unknown, which makes determining the pressure rating difficult. Current inspection techniques address some of these issues, but they are not comprehensive. This paper will briefly discuss current inspection techniques and relevant literature for relating nondestructive measurements to key strength and toughness properties. A project is in progress to provide new in-trench tools that will give strength properties without the need for sample removal and destructive testing. Preliminary experimental ultrasonic methods and measurements will be presented, including velocity, attenuation, and backscatter measurements.

Keywords

Materials properties, Mechanical stress, Educational assessment

Disciplines

Mechanics of Materials | Structural Materials

Nondestructive characterization of pipeline materials

Cite as: AIP Conference Proceedings **1650**, 943 (2015); https://doi.org/10.1063/1.4914700
Published Online: 02 April 2015

Brady J. Engle, Lucinda J. Smart, and Leonard J. Bond

Nondestructive Characterization of Pipeline Materials

Brady J. Engle[*,†], Lucinda J. Smart[*] and Leonard J. Bond[*]

[*]*Center for Nondestructive Evaluation, Iowa State University, Ames, IA*
[†]*Corresponding Author: bjengle@iastate.edu*

Abstract. There is a growing need to quantitatively and nondestructively evaluate the strength and toughness properties of pipeline steels, particularly in aging pipeline infrastructure. These strength and toughness properties, namely yield strength, tensile strength, transition temperature, and toughness, are essential for determining the safe operating pressure of the pipelines. For some older pipelines crucial information can be unknown, which makes determining the pressure rating difficult. Current inspection techniques address some of these issues, but they are not comprehensive. This paper will briefly discuss current inspection techniques and relevant literature for relating nondestructive measurements to key strength and toughness properties. A project is in progress to provide new in-trench tools that will give strength properties without the need for sample removal and destructive testing. Preliminary experimental ultrasonic methods and measurements will be presented, including velocity, attenuation, and backscatter measurements.

INTRODUCTION

It is crucial that pipelines be operated at safe pressures to prevent failure. In order to enable assessments to be made and ensure the operating pressure is safe, flaws need to be detected and the strength properties of the pipeline material, particularly yield strength, tensile strength, ductile-to-brittle transition temperature, and toughness should be determined. In the wake of the 2010 natural gas pipeline accident in San Bruno, CA, the National Transportation Safety Board identified in-line inspection (ILI) tools as the most effective technique for flaw detection in pipelines and recommended that all older gas transmission lines be modified so that ILI tools can be used [1]. Such tools currently provide details for in-pipe defects. If ILI tools could determine strength and toughness properties in addition to flaw detection, then they could help identify areas of pipe that may be more susceptible to flaw initiation. In the case of the San Bruno accident, not only was a flaw present, but several sections of the failed pipeline had substandard yield strength [1]. For some older pipelines this strength information can be unknown due to insufficient testing or record keeping. Limited information about strength and toughness properties can be obtained with current technology through the use of ILI tools and various in-the-ditch measurements, which require the pipeline to be dug up and exposed. These properties can be obtained destructively by cutting a sample from the pipeline and performing tests on it, though this is not an ideal solution since it introduces a stress concentration and local anomaly to the pipeline.

This paper is part of a larger project which has the goal of providing a proof-of-concept that nondestructive techniques can be used to estimate yield strength, tensile strength, transition temperature, and toughness for pipeline steels. The paper will review the state-of-the art for inspection technologies currently in use in the pipeline industry before presenting some preliminary ultrasonic measurements on actual pipeline samples. An overview of results to-date and plans for future work are discussed.

Current Inspection Technology

In-Line Inspection Tools. In-line inspection (ILI) tools are commonly used for pipeline inspections. ILI tools are placed inside the pipeline and pushed along by the flow inside the pipe. These tools include one or more sensors, primarily ultrasonic and electromagnetic, that can measure metal loss, detect cracks, and determine pipe geometry [2]. These tools focus mainly on defect detection, while providing little information about the pipeline material itself.

In-the-Ditch Techniques. If the pipeline has been excavated, several tests can be done. Chemical testing can be done to determine the chemical composition of the steel. Hardness measurements can be performed, which can then

41st Annual Review of Progress in Quantitative Nondestructive Evaluation
AIP Conf. Proc. 1650, 943-951 (2015); doi: 10.1063/1.4914700

be used to look for correlations with other material properties. Sections of the outer surface of the pipe can be polished and etched allowing for microscopic measurements to be made.

Destructive Methods. Pipelines can undergo hydrostatic testing, which fills the line with a fluid pressurized to some specified pressure. If the pipeline has flaws, hydrostatic testing may cause the line to rupture. Samples can be removed from the pipeline and destructively tested to determine material properties. Measurements from yield and tensile tests can determine the strength of a sample. Charpy impact testing can be used to destructively determine fracture toughness and can be used to find the ductile-to-brittle transition temperature.

NONDESTRUCTIVE MEASUREMENTS FOR MATERIAL PROPERTY DETERMINATION

There has been work in the past showing relationships between measured ultrasonic properties and material properties, including both microstructural properties like grain size and strength properties. Freitas [3] showed that ultrasonic velocity and attenuation are sensitive to varying microstructures in steels, and Vary [4] found a relationship between elastic moduli and wave velocity. Stanke and Kino [5] showed the theoretical relationship between ultrasonic attenuation and grain size, and Palanichamy [6] showed an experimental relationship between velocity and grain size for stainless steel. Margetan [7] explains how backscattered grain noise can be related to various microstructural properties.

Preliminary Ultrasonic Measurements

To investigate if any similar relationships are present within our sample set, a variety of ultrasonic properties were measured:

- longitudinal wave velocity,
- attenuation, and
- backscattered grain noise.

An initial set of samples was provided by our industry partners with the goal of providing samples that had varying strength and toughness properties. Of these, the grain size was known for three samples, and details are shown in Table 1. The qualitative grain size relationship between the samples is A>C>B, with values shown in Table 1. Initial ultrasonic measurements were carried out to determine if any strong relationships between the ultrasonic properties and the strength and toughness properties could be found. Each sample had multiple zones for which measurements were carried out. The original plan was to inspect three zones per sample. Sample A had a very uniform shape and surface, so an extra zone was included to help quantify the degree of variability within this sample. Sample B only has two zones due to curvature issues that are discussed later on in this paper. The wall thickness for each zone is shown in Table 2. These samples were inspected using a normal-incidence water immersion setup with a 20 MHz, 1/8" diameter planar transducer. Examples of the data collected are shown in Fig. 1. On the left is a saturated front wall signal followed by a series of back wall echoes. On the right is the same series of signals (collected at a different time; note the differing front wall arrival times), but at much higher gain. Grain noise can be seen between the front wall and several subsequent echoes in this figure.

TABLE 1. Samples chosen for initial measurements.

Sample	Grade	Outer Diameter (in)	Yield Strength (psi)	Tensile Strength (psi)	Percent Ferrite	Transition Temp. ($^\circ$ F)	ASTM Grain Size No.	Mean Grain Size (μm)
A	B	6.5	58000	74000	72.7	120	11.009	7.9
B	X42	8.75	70000	86000	68.5	-24	12.707	4.4
C	X46	16	51500	65500	78.7	119	11.557	6.5

TABLE 2. Sample thicknesses (cm).

	Sample A	Sample B	Sample C
Zone 1	0.516 cm	0.759 cm	0.683 cm
Zone 2	0.508 cm	0.752 cm	0.686 cm
Zone 3	0.503 cm		0.671 cm
Zone 4	0.505 cm		

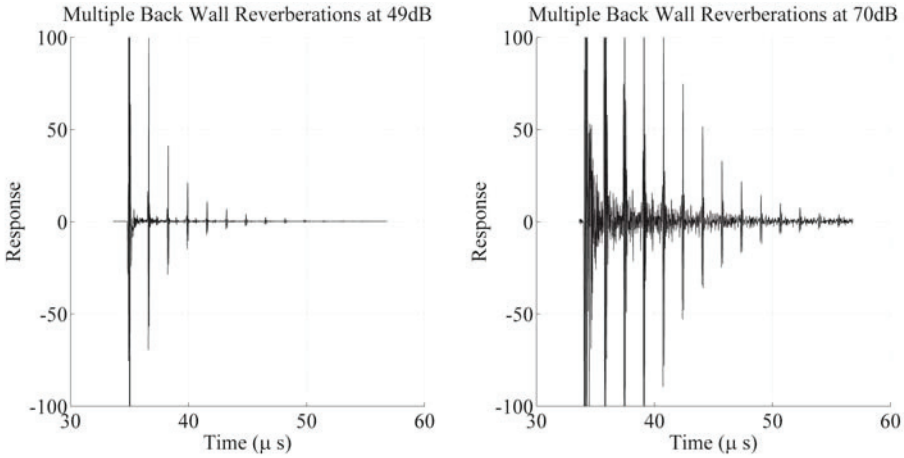

FIGURE 1. Front wall signal with multiple back wall reverberations. Gain set at 49 dB (left) and 70 dB (right).

Velocity

The velocity was estimated using the arrival times of six back wall echoes for each zone in each sample. An example waveform showing the multiple back wall reverberations was shown in Fig. 1. The positive peaks of each back wall echo were measured and plotted against the propagation distance of each echo, which is known using the thickness measurements in Table 2. A line was fit to this data, and the slope was taken to be the velocity. These

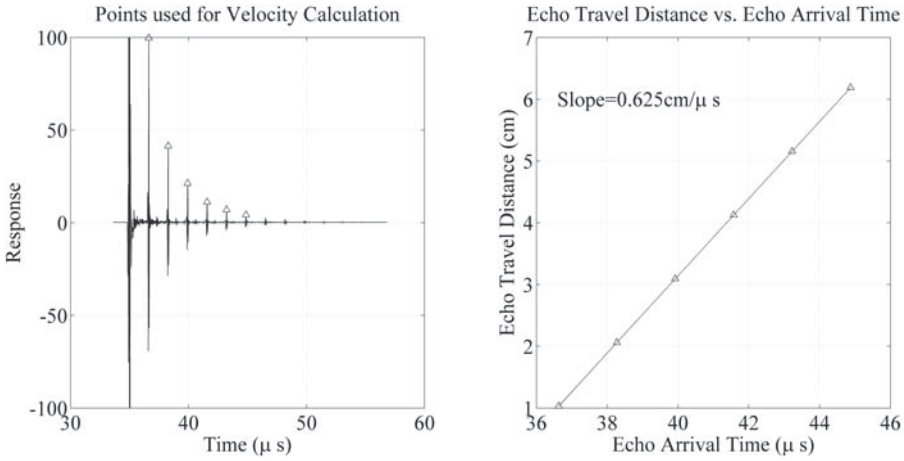

FIGURE 2. Velocity calculation for Sample A zone 1. The left plot shows the points used to determine the arrival time of each back wall echo. The right plot shows these times plotted against the wave travel distance, with a line fit to the data whose slope is the velocity.

steps are illustrated in Fig. 2, where the triangles in the left plot denote the positive peaks whose arrival times were

used. The triangles in the right plot correspond to these same arrival times. This process was done for all zones of each sample, and the results can be seen in Fig. 3. The mean velocity results for the three samples, given in Table 3,

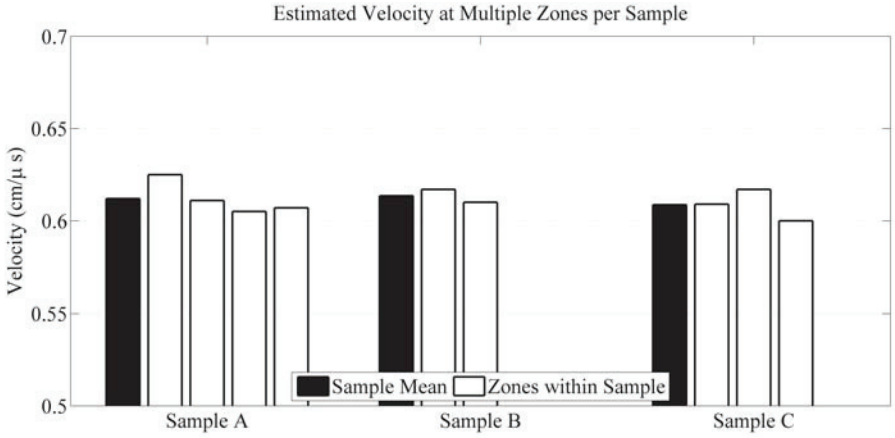

FIGURE 3. Longitudinal velocity results for each sample. Sample means are black bars, individual zones are white bars.

were within 0.005 $cm/\mu s$ of each other. Said another way, the fastest velocity is only 0.5% higher than the slowest

TABLE 3. Mean velocities for each sample.

	Sample A	**Sample B**	**Sample C**
Mean Velocity (cm/μs)	0.612	0.614	0.609

velocity. Within a sample, however, much greater variation can be seen. For example, zones one and three of sample A differ by about 0.020 $cm/\mu s$. When looking only at the mean values, some preliminary correlations can be made between the velocity and known parameters of our sample set, particularly yield strength, tensile strength, and percent ferrite. These correlations are made for discussion purposes; the velocity variation in each sample, which is denoted by bars indicating plus or minus one standard deviation of the variation in a sample, is too large to have confidence in these relationships. The correlation between velocity and yield strength can be seen in Fig. 4. Figure 4 shows

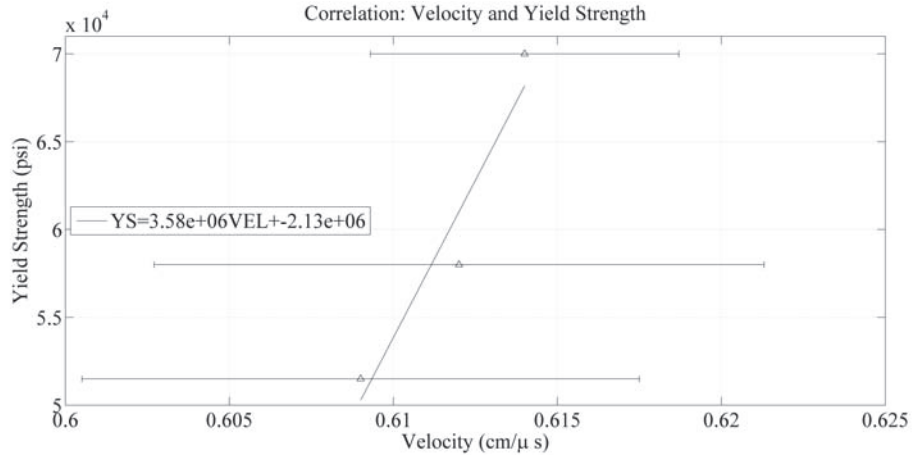

FIGURE 4. Relationship between velocity and yield strength. Bars represent plus/minus one standard deviation of variation within sample.

that, for this data, yield strength increases as velocity increases. A similar relationship is found between velocity and tensile strength, shown in Fig. 5. These relationships between velocity and strength were not expected, and analogous

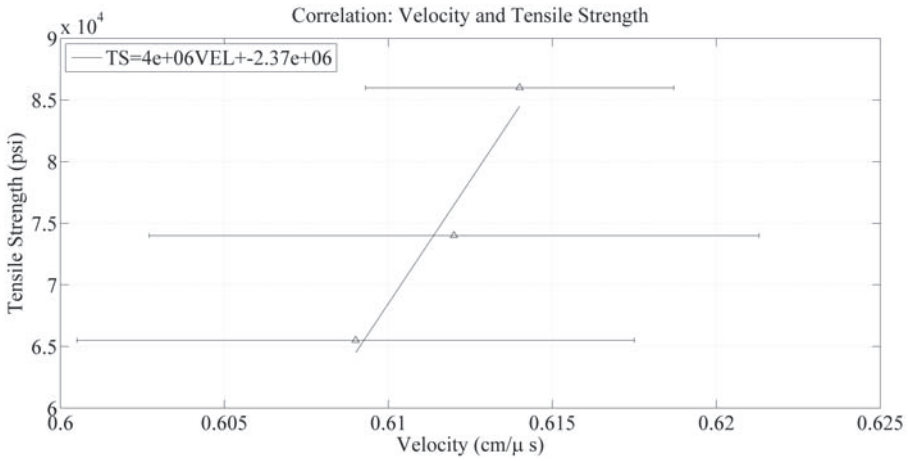

FIGURE 5. Relationship between velocity and tensile strength. Bars represent plus/minus one standard deviation of variation within sample.

relationships have not been seen during the literature review. Due to the small number of samples tested, there is no guarantee that these relationships will hold once more samples are tested. For example, according to the Hall-Petch relationship, yield strength should increase with decreasing grain size. Of the three samples tested, which have the grain size relationship A>C>B, sample B has the highest yield strength, followed by Sample A, and then Sample C. This means that this set of three samples does not qualitatively follow the Hall-Petch relationship. Because of this anomalous behavior regarding the Hall-Petch relation, the relationships shown between velocity and yield and tensile strength could themselves be anomalous and not present themselves once more samples have been tested.

The third relationship that can be seen from this data is between velocity and percent ferrite, shown in Fig. 6. Figure 6

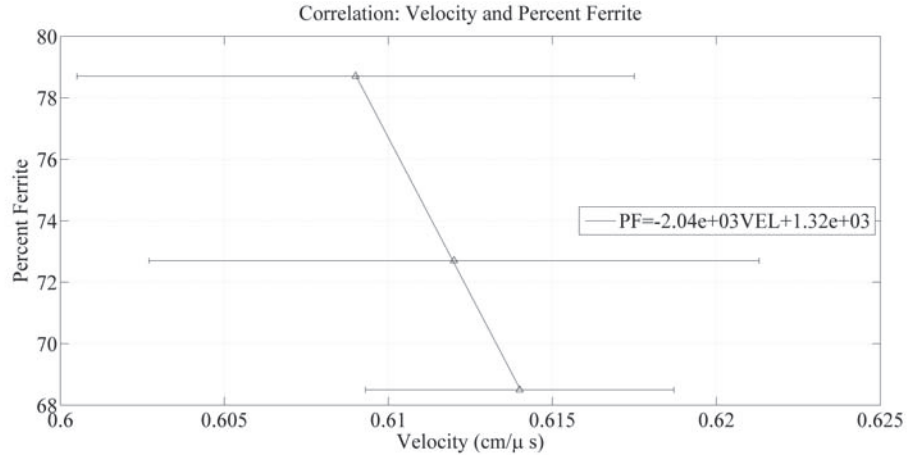

FIGURE 6. Relationship between velocity and percent ferrite. Bars represent plus/minus one standard deviation of variation within sample.

shows that velocity increases with decreasing ferrite content. All three samples have a ferrite-pearlite microstructure, and the ferrite percentage is a parameter used to estimate the ratio between the ferrite and pearlite. Gür and Tuncer [9] found for all of the steels that they tested that lower ferrite content corresponds to lower velocity, which is the opposite of what is shown in Fig. 6. Gür and Tuncer note that for pearlite-ferrite microstructures the lamellae spacing is a key factor that influences ultrasonic velocity, which is a parameter not taken into account in this paper.

Attenuation

The attenuation in these samples was calculated as the frequency domain ratio of the second back wall echo to the first back wall echo. Each back wall signal is thought of as [8]

[Measured Signal] = [System Efficiency] x [Interface Effects] x [Diffraction] x [Attenuation] (1)

which, in words, states that the measured signal is the convolution of the effects of the ultrasonic system, the reflection and transmission at interfaces, the spread of the beam while propagating, and the attenuation. Using the ratio of the second back wall signal to the first, the system efficiency term will cancel out, and the interface and diffraction terms can be modeled. This allows for the attenuation $\alpha(f)$ to be calculated [8].

Curves of attenuation as a function of frequency were calculated for each zone of each sample. Within a sample, mean curves were created by averaging the curves from each zone together. These mean curves can be seen in Fig. 7. The frequency range over which we will consider these attenuation estimates as valid is roughly 5-20 MHz. The

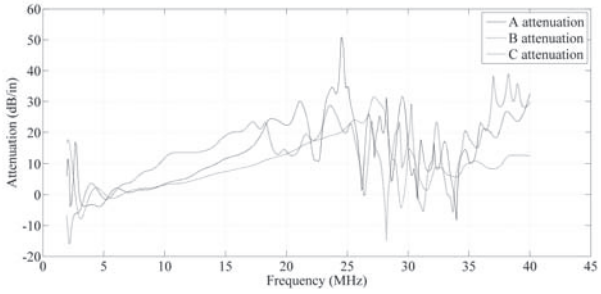

FIGURE 7. Mean attenuation results for each sample. Bandwidth for reliable data estimated to be 5-20 MHz.

results for each sample are shown in Fig. 8. Figure 8 shows very large variations in attenuation within the samples. For example, in the 10 MHz plot (left) the fourth zone of Sample A has attenuation nearly four times that of the second zone in the same sample. At this preliminary stage it is difficult to judge how much of this variation is actually due to varying attenuation within the samples and how much variation is due to the experiment itself. Sample B is from a curved section of pipeline; its longitudinal axis has curvature. This curvature manifested itself in Zone 2 of Sample B as a very weak second back wall signal. When coupled with the cylindrical shape of the sample, this additional curvature created a complex shape which was not accounted for in the attenuation model, leading to a very weak back surface signal. The weak back wall signal gives the impression of very high attenuation, even though much of the energy loss is likely due to the unaccounted-for complex curvature. Data was not collected for additional zones of Sample B since the validity of the data would be questionable.

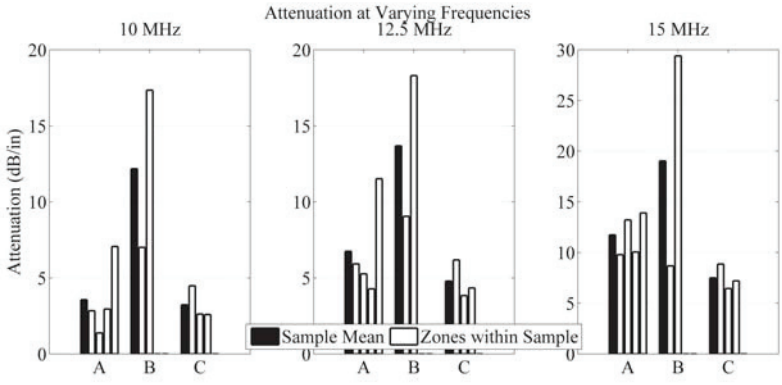

FIGURE 8. Attenuation results for 10 MHz (left), 12.5 MHz (center), and 15 MHz (right). Black bars correspond to mean values for each sample. White bars are individual zones for each sample.

Attenuation is a promising quantity for relationships with grain size and strength and toughness properties, but correlations cannot be justified with only two data points since the data from Sample B is being considered invalid due to curvature issues.

Backscattered Grain Noise

To measure backscattered grain noise in the samples a scan was performed over a region 1.27 centimeters long in the axial direction while rotating the sample twenty degrees. Step sizes in the respective dimensions were 0.0254 centimeters and 0.5 degrees. Waveforms were collected at high gain for each point in the scan, and an example was shown in Fig. 1. There is grain noise present in between the front and back wall signals, which can be seen in Fig. 9, but it is difficult to determine a region that shows grain noise that is not being masked by the large front wall decay. To get a measure of backscattered grain noise, all of the waveforms from a scan were spatially averaged to get what we will call V_{rms}. This quantity is calculated as

$$V_{rms}(t) = \left[\frac{1}{M} \sum_{j=1}^{M} (V_j(t) - V_{avg})^2 \right]^{1/2} \tag{2}$$

where

$$V_{avg} = \frac{1}{M} \sum_{j=1}^{M} V(j). \tag{3}$$

A mean V_{rms} curve was made for each sample using the data from the different zones within the sample. Curves for all three samples can be seen in Fig. 10. These curves show a large front wall signal that decays until the back wall signal occurs. In an effort to look at V_{rms} at different depths in the material, values were taken from the V_{rms} curves at specific

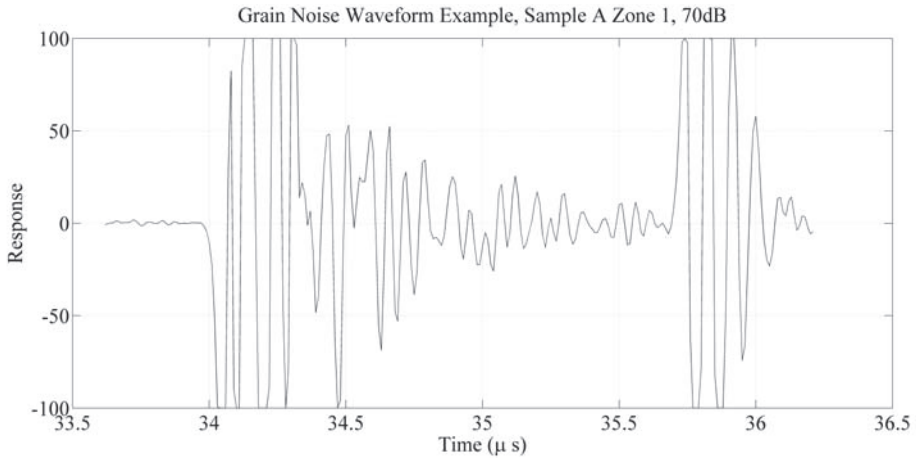

FIGURE 9. Waveform taken from Sample A, zone 1 at 70 dB gain. Saturated front and back wall signals are shown with grain noise in between.

time intervals after the front wall signal surpassed some chosen threshold. Figure 11 shows these values for individual zones as well as the mean values for each sample for 1 and 1.5 microseconds after the front wall signal hits a value of twenty. Because the onset of the front wall signal does not correspond to the actual time-of-flight of the front surface it is difficult to relate 1 and 1.5 microseconds to absolute depths into the samples, but they do correspond to points on the curve when the front wall signal has mostly decayed. As with the attenuation results, the variation seen within a sample can be much larger than the variation between the means of the samples. The main relationship involving grain noise is expected to be with grain size, and looking qualitatively just at the mean results, the sample with the largest grains, Sample A, has the largest response, which is the expected result. It would be expected that Sample C would have a larger response than Sample B since Sample C has larger grains, but the opposite result is seen. The three samples have varying degrees of surface rougness, which could potentially skew these results. When comparing amplitude

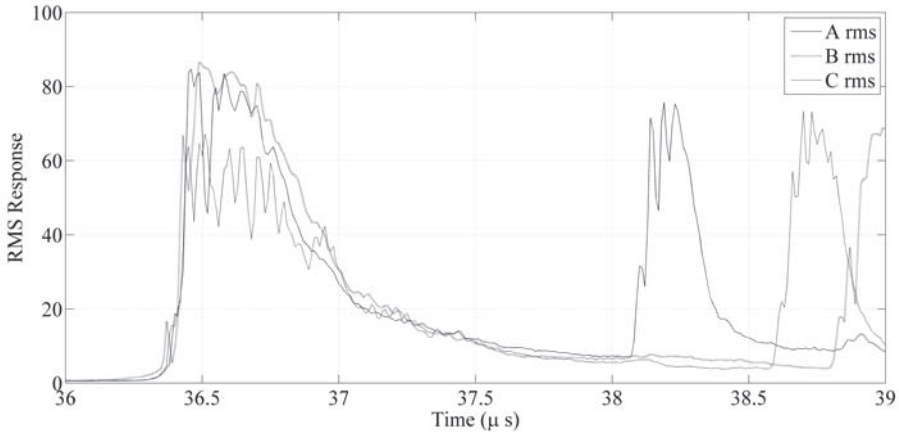

FIGURE 10. Mean V_{rms} curves for each sample.

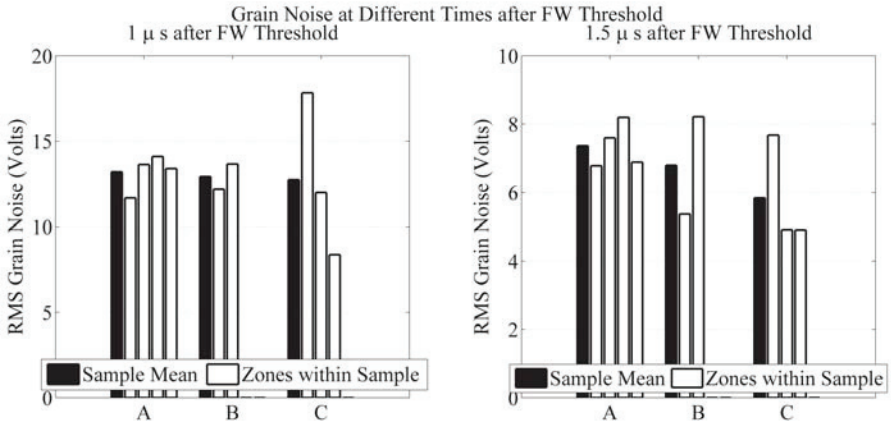

FIGURE 11. Grain noise results for 1 μs (left) and 1.5 μs (right) after the front wall V_{rms} signal passes a threshold. Black bars correspond to mean values for each sample. White bars are individual zones for each sample.

results between samples like what is being done here, a rough surface may prevent as much energy from entering the sample than would enter if the surface was smooth. Therefore, less energy would be scattered by the grains, and the RMS response would be lower overall. Regardless, the methodology developed so far is a strong foundation for the determination of grain size using backscattered grain noise and will continue to be refined.

CONCLUSIONS AND FUTURE WORK

Preliminary ultrasonic measurements were made on an initial sample set to test and demonstrate the proposed measurement modality and to determine velocity, attenuation, and backscattered grain noise. The hypothesis being tested is that these quantities would have strong relationships with microstructural properties such as grain size as well as mechanical properties, particularly yield strength, tensile strength, ductile-to-brittle transition temperature, and toughness. The results up to this point, however, are inconclusive. The initial sample set contained samples that had varying degrees of curvature and surface roughness, which weren't taken into account in the attenuation and backscattered grain noise analysis. The results do demonstrate a measurement methodology, but showed large

variation within samples, and it is difficult to determine how much variation is due to actual material differences or whether factors such as the curvature and roughness are skewing the results. Because of this, correlations were not attempted for the attenuation and grain noise results. Correlations were made for velocity with yield strength, tensile strength, and percent ferrite, though they were unlike what was seen in the literature.

Moving forward, several steps will be taken to improve and build on this work. A larger sample set will be acquired, with two goals in mind: firstly, the samples should be different enough microstructurally to demonstrate that the ultrasonic measurements can clearly distinguish between them, and secondly, the samples will have more information known regarding their composition and microstructure so that relationships can be more easily noted between the ultrasonic measurements, microstructural properties, and strength/toughness properties. Once the samples have been acquired, steps will be taken to ensure that the surface conditions are consistent between samples, and the experimental methodologies will be refined.

ACKNOWLEDGMENTS

This work is supported by the Competitive Academic Agreement Program of the United States Department of Transportation Pipeline and Hazardous Materials Safety Administration in collaboration with Applus RTD, Kiefner and Associates, and the Pacific Gas and Electric Company.

REFERENCES

1. National Transportation Safety Board. 2011. *Pacific Gas and Electric Company Natural Gas Transmission Pipeline Rupture and Fire, San Bruno, California, September 9, 2010.* Pipeline Accident Report NTSB/PAR-11/01. Washington, DC.
2. Barbian, A., and M. Beller. 2012. "In-Line Inspection of High Pressure Transmission Pipelines: State-of-the-Art and Future Trends." 18th World Conference on Nondestructive Testing, Durban, South Africa.
3. Freitas, V. L. de A., V. H. C. de Albuquerque, E. de M. Silva, A. A. Silva, and J. M. R. S. Tavares. (2010) Nondestructive Characterization of Microstructures and Determination of Elastic Properties in Plain Carbon Steel Using Ultrasonic Measurements. Materials Science and Engineering: A 527.16: 4431-4437.
4. Vary. A. (1980) Ultrasonic Measurement of Material Properties. In Research Techniques in Nondestructive Testing, Vol. IV. R. S. Sharpe, ed. Academic Press (London). pp. 159-204.
5. Stanke, F. E., and G. S. Kino. "A unified theory for elastic wave propagation in polycrystalline materials." The Journal of the Acoustical Society of America 75.3 (1984): 665-681.
6. Palanichamy, P., A. Joseph, T. Jayakumar, and B. Raj. "Ultrasonic velocity measurements for estimation of grain size in austenitic stainless steel." NDT & E International 28.3 (1995): 179-185.
7. Margetan, F. J. "Bruce Thompson: Adventures and advances in ultrasonic backscatter." in Review of Progress in Quantitative Nondestructive Evaluation, Vol. 31, 1430, edited by D. O. Thompson and D. E. Chimenti, published by AIP, Melville, NY, 2012, pp. 1234-1235.
8. Margetan, F. J., D. J. Barnard, D. L. Orman, A. Feygin, and B. Pavel. "A web-based tutorial for ultrasonic attenuation measurement." in Review of Progress in Quantitative Nondestructive Evaluation, Vol. 33, 1581, edited by L. J. Bond, D. E. Chimenti and D. O. Thompson, published by AIP, Melville, NY, 2014, pp. 2127-2134.
9. Gür, C. H., and B. O. Tuncer. "Characterization of microstructural phases of steels by sound velocity measurement." Materials Characterization 55.2 (2005): 160-166.